

PROGRESS ON THE USE OF COMBINED ANALOG AND PHOTON COUNTING DETECTION FOR RAMAN LIDAR

Rob Newsom¹, Dave Turner², Marian Clayton³, Richard Ferrare⁴

¹Pacific Northwest National Laboratory, P.O.Box 999, MSIN K9-30, Richland, WA, 99352, USA,
rob.newsom@pnl.gov

²University of Wisconsin, Madison, WI, USA, dturner@ssec.wisc.edu

³SAIC/NASA Langley Research Center, Hampton, VA, USA, marian.f.clayton@nasa.gov

⁴NASA Langley Research Center, Hampton, VA, USA, richard.a.ferrare@nasa.gov

ABSTRACT

The Atmospheric Radiation Measurement (ARM) program Raman Lidar (CARL) was upgraded in 2004 with a new data system that provides simultaneous measurements of both the photomultiplier analog output voltage and photon counts. The so-called merge value added procedure (VAP) was developed to combine the analog and count-rate signals into a single signal with improved dynamic range. Earlier versions of this VAP tended to cause unacceptably large biases in the water vapor mixing ratio during the daytime as a result of improper matching between the analog and count-rate signals in the presence of elevated solar background levels. We recently identified several problems and tested a modified version of the merge VAP by comparing profiles of water vapor mixing ratio derived from CARL with simultaneous sonde data over a six month period. We show that the modified merge VAP significantly reduces the daytime bias, and results in mean differences that are within approximately 1% for both nighttime and daytime measurements.

1. INTRODUCTION

The Raman lidar (CARL) at ARM's Southern Great Plains site is an autonomous, turn-key system [1] that has been operational now for 10 years. The system transmits at a wavelength of 355 nm with 300 mJ, 20 ns pulses, and a pulse repetition frequency of 30Hz. The detection system currently consists of 10 channels each with range resolutions of 7.5m. These include 2 water vapor channels at 408 nm, 2 nitrogen channels at 387nm, 3 elastic channels, two temperature channels at 354 and 353nm, and one liquid water channel [1]. The lidar has two fields-of-view (FOV), where in the wide field of view there are three channels (water vapor, nitrogen, and elastic) with a 2 mrad FOV, and the remaining the channels have a 0.3 mrad FOV. Data products derived from CARL include water vapor mixing ratio, aerosol scattering ratio, aerosol extinction, and linear depolarization ratio [2].

In 2004 the system underwent a major upgrade. As part of this upgrade the existing data system was replaced with new transient data recorders from Licel GbR (Berlin, Germany). The Licel recorders offer the

advantage of increased dynamic range by providing simultaneous measurements of both analog photomultiplier current and photon counts. The new detection electronics enable water vapor profiling up to 5-6 km AGL during the day, which is a marked improvement over the original version of this lidar (~3 km in 1999). In order to take advantage of this capability, the so-called merge VAP was developed to combine the analog and count-rate signals into a single signal with improved dynamic range. This VAP represents the first critical step in the data processing chain for CARL.

Earlier versions of the merge VAP resulted in large biases in daytime mixing ratios. As a result, this VAP was never implemented operationally within ARM's data management facility, and with time the backlog of unprocessed raw data grew. Thus, the problem was recently elevated to critical status by the ARM community, and an intensive effort was launched to identify and remedy the problem in the merge VAP. This paper summarizes those efforts and the modifications that have been made which have resulted in a significant reduction of the daytime mixing ratio biases.

2. MERGE ALGORITHM BASICS

The first step in the merge process involves correcting the count-rate signal for pulse pileup effects. Assuming that the PMT and associated electronics obey the nonparalyzable assumption [3], this correction takes the following form:

$$C'_{ij} = \frac{C_{ij}}{1 - \tau C_{ij}}, \quad (1)$$

where C_{ij} is the measured count rate, and τ is the deadtime parameter. The indices i and j are used to denote time and height such that $C_{ij} = C(t_i, z_j)$.

Above its inherent noise floor the analog signal is assumed to be proportional to the "true" count rate. The so-called virtual count rate is defined as

$$\hat{C}_{ij} = s_i A_{ij} + o_i, \quad (2)$$

where A_{ij} is the analog signal. The slope, s_i , and offset, o_i , are referred to as the glue coefficients (GC's). A single set of GC's are determined for each profile. Thus, s_i , and o_i are, in general time-dependent and height-independent.

The merged signal is obtained by combining the virtual and corrected count rate data such that

$$C_{ij}^{merge} = \begin{cases} C'_{ij} & \text{for } C'_{ij} < C_{max} \\ \hat{C}_{ij} & \text{for } C'_{ij} \geq C_{max} \end{cases}, \quad (3)$$

where C_{max} is a prescribed transition threshold. The merged signal incorporates the superior sensitivity of the count rate data in the weak signal regime, and the improved linearity of the analog data in the strong signal regime.

2.1 Glue Coefficients

The GC's are determined by linear regression while constraining the fit range. In the regression the range of C'_{ij} is restricted such that

$$C_{bi} + \delta C < C'_{ij} < C_{max}, \quad (4)$$

where C_{bi} is the mean count rate of the solar background, and δC is a prescribed parameter that determines the lower threshold relative to the solar background. In our current implementation we use $\delta C = 0.5$ MHz. This helps to suppress the impact of the background signal in the regression.

The upper limit of the fit range is determined by the transition threshold, C_{max} . It is necessary to impose this limit because equation (1) represents an approximation that is only applicable for small signals, i.e. for $\tau C_{ij} \ll 1$. Thus, C_{max} should be set to a small value in order to satisfy this condition. However, C_{max} must also be large enough to ensure an adequate fit range for the regression. These two conflicting requirements create problems for the determination of the GC's during the daytime for the solar-sensitive channels. As the solar background increases during the daytime the fit range is reduced. This is particularly problematic for the water vapor channel since this channel exhibits the greatest sensitivity to solar radiation.

In our current implementation we use $C_{max} = 50$ MHz.

Even with this relatively large value of C_{max} there are long periods during the day when $C_{bi} + \delta C \geq C_{max}$ for the water vapor channel. During these periods it is not possible to derive the GC's. We are forced instead to simply interpolate through the daytime voids, as illustrated in Figure 2.

2.2 Analog signal delay

One potential pitfall associated with the use of the Licel data recorders is the inherent phase shift of the analog signal with respect to the count-rate signal. Electronic processing of the analog signal induces a slight delay relative the count-rate signal. If this shift is not properly account for it can adversely affect C_{ij}^{merge} .

Licel units were installed in all of the existing detection channels as part of the major upgrade in 2004. All of these original units produced the same delay or phase shift, i.e. the analog signal was delayed by 3 range bins (~ 150 ns) relative to the count rate signal. The following year three new channels (and three new Licel units) were added for temperature and liquid water profiling [4]. These newer Licel units produced delays of 8 range bins (~ 400 ns). However, the difference was not immediately detected and the merge code continued to assume a shift of three bins for all channels. This problem has since been fixed and we have made it standard practice to check the phase shift whenever a new Licel unit is added to the system or when units are swapped between detection channels.

3. BASELINE VS MODIFIED MERGE VAPS

3.1 Regression method

In the original or baseline implementation the GCs are determined from a linear regression between \hat{C}_{ij} and C'_{ij} . This is equivalent to minimizing

$$J = \sum_j \frac{(C'_{ij} - \hat{C}_{ij})^2}{\sigma_{ij}^2} \quad (5)$$

with respect to s_i , and o_i . The measurement error is assumed to be proportional to the count-rate. Therefore, we set $\sigma_{ij} = C'_{ij}$.

In the baseline merge VAP the GCs are determined by treating C'_{ij} as the dependent variable in the linear regression, while truncating its range according to equation (4). This truncation can cause biases in the GCs when there is significant scatter in the data, as

illustrated in Figure 1. This problem has been addressed in the modified merge VAP by simply reversing the roles of the analog and count-rate data in the linear regression. In this approach the count-rate data are treated as the independent variable. Thus, in the modified merge VAP the GC's are obtained by minimizing

$$J = \sum_j \frac{(A_{ij} - (s'_i C'_{ij} + o'_i))^2}{\sigma_{ij}^2} \quad (6)$$

with respect to s'_i and o'_i . Here, the measurement error is assumed to be proportional to the analog signal. Once s'_i and o'_i are determined, the GC's are computed from $s_i = 1/s'_i$ and $o_i = -o'_i s_i$. These results are then used to compute the virtual count-rate, \hat{C}_{ij} . The signals are then merged, as in the baseline method, using equation (3).

Figure 1 illustrates the effect that this modification has on the virtual count rate, \hat{C}_{ij} . This particular example shows results from the wide-field-of-view water vapor channel during a late morning period on 16 August 2007. The baseline regression method clearly produces slopes that are biased toward lower values as a result of the truncation in the dependent variable.

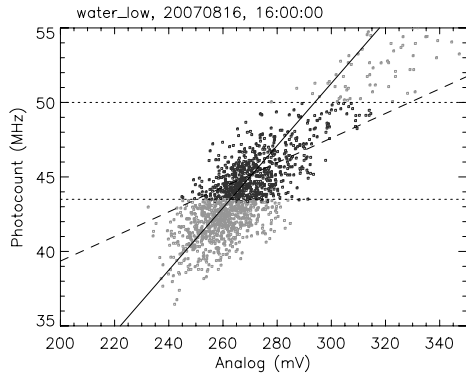


Figure 1. Solid and dashed lines show the virtual count-rate as functions of the analog signal for the modified and baseline merge algorithms, respectively. The darker points fall within the fit region as defined by equation (4).

Figure 2 shows time series of the slope, s_i , for the baseline and modified merge VAPs. The modified merge VAP exhibits much less sensitivity to changing solar background. In fact, Figure 2b suggests that a simple approach based on the use of constant GC's may be adequate to describe the virtual count-rate.

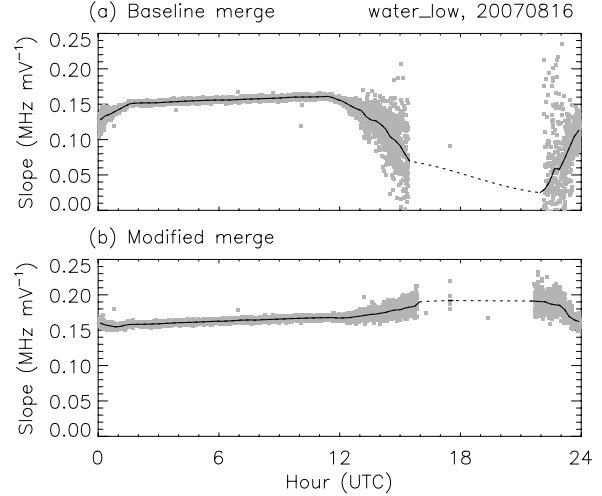


Figure 2. Time series of the slope, s , for (a) the baseline merge VAP, and (b) the modified merge VAP. These examples were taken from the wide-field-of-view water vapor channel on 16 August, 2007. The solid lines are obtained by smoothing the beam-to-beam slopes (gray dots). The dotted lines are obtained by linear interpolation of the smoothed slopes.

3.2 Determination of τ

For the modified merge VAP the deadtime parameters are estimated by applying a slight generalization of the regression technique discussed in section 3.1. The generalization involves minimizing equation (6) with respect to s'_i , o'_i and τ . In this approach we seek the value of τ that results in the best linear fit between \hat{C}_{ij} and C'_{ij} over fit range defined by equation (4). The deadtime parameter obtained using this technique is consistent with the regression method that is used to determine the GC's. Additionally, this technique is applied using data from an entire diurnal cycle. This permits us to estimate τ for the water vapor channel by taking advantage of the range of signal caused by the changing solar background.

4. WATER VAPOR MIXING RATIO

This section presents comparisons of lidar derived water vapor mixing ratios to simultaneous radiosonde measurements. Raw lidar data were processed using the baseline and modified merge VAP over a six month period from 1 April to 30 September 2007. The output from these VAPs were then processed using the same code (rlprof_mr) to generate two different mixing ratio data sets. For these comparisons the modified merge VAP was configured to use only the nighttime average GC's, while the baseline merge VAP used diurnally varying GC's.

Figures 4 and 5 show profiles of the average ratio of the lidar to sonde mixing ratio derived from the baseline and modified merge VAPs, respectively. Sonde humidity data were scaled with a height-independent factor in order to force agreement with measurements of precipitable water vapor (PWV) from a nearly colocated microwave radiometer. This helped to largely remove any diurnal bias in the radiosonde humidity profile [5]. Only soundings during clear periods were used in the comparisons. Daytime and nighttime profiles were separately averaged based on the solar background level in the wide-field-of-view water vapor channel. There were a total of 157 daytime and 143 nighttime soundings used in these comparisons.

Both the baseline (Fig 3) and modified (Fig 4) merge VAPs produced mixing ratios that agree with the sonde data to within approximately 1% during the nighttime. However, the baseline merge VAP exhibits a difference of about 4% between the daytime and nighttime bias. By contrast, difference between the daytime and nighttime biases for the modified merge VAP is about 1%.

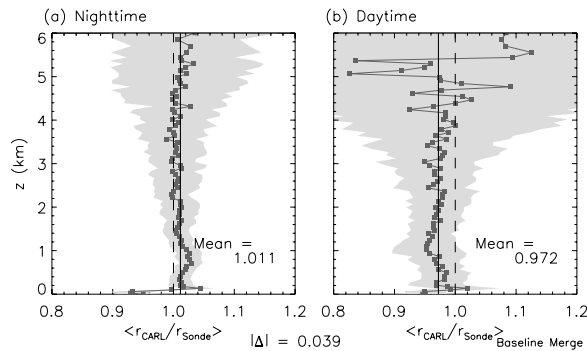


Figure 3. Results using the baseline merge VAP. Profiles of the average ratio of the CARL-to-sonde mixing ratio for (a) nighttime and (b) daytime soundings. The solid lines indicate the value of the vertically averaged CARL-to-sonde ratio.

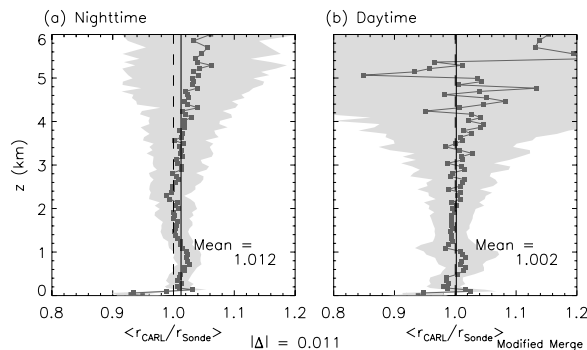


Figure 4. Results using the modified merge VAP. Profiles of the average ratio of the CARL-to-sonde mixing ratio for (a) nighttime and (b) daytime soundings. The solid lines indicate the vertically averaged CARL-to-sonde ratio.

5. SUMMARY

Recent modifications to the so-called merge VAP have been shown to reduce the daytime biases in mixing ratios derived from CARL. The CARL and sonde mixing ratios are in agreement to within approximately 1% on average for both nighttime and daytime measurements. These modifications enable operational processing of the Raman lidar to begin, thus removing the bottleneck in the data processing chain that has existed since the new data system was installed in 2004. The modified version of the merge VAP is currently in production within the data management facility at Pacific Northwest National Laboratory and merge data are being generated and made available to the user community through the Atmospheric Radiation Measurement program web site (<http://www.arm.gov/>).

Acknowledgements

We would like to thank Dr. John Goldsmith, Sandia National Laboratories, for his invaluable expertise and continuing assistance with the lidar hardware. We would like to thank Bernd Mielke, Licel GbR, for his help with the Licel electronics and Diana Petty for helping to lay the ground work for the merge algorithm. We would also like to thank Chris Martin, SGP Site Operations, for the day-to-day maintenance of CARL. CARL is operated by the ARM Program and is sponsored by the US Department of Energy, Office of Energy Research, Office of Health and Environmental Research, Environmental Science Division.

REFERENCES

- [1] Goldsmith J. E. M., F. H Blair, S. E. Bisson, D. D. Turner, 1998: Turn-key Raman lidar for profiling atmospheric water vapor, clouds and aerosols, *Appl. Optics*, **37**, pp. 4979-4990.
- [2] Turner D. D., et al., 2002: Automated retrievals of water vapor and aerosol profiles from an operational Raman lidar, *J. Atmos. Oceanic Technol.*, **19**, pp. 37-49.
- [3] Whiteman D. N., S. H. Melfi, R. A. Ferrare, 1992: Raman lidar system for the measurement of water vapor and aerosols in the Earth's atmosphere, *Appl. Optics*, **31**, pp. 3068-3082.
- [4] Petty D., D. D. Turner, J. Goldsmith, J. Comstock, Z. Wang, 2006: Eight years of continuous Raman lidar measurements of water vapor, aerosol and clouds over the southern Great Plains, Raman lidar measurements, *Preprints of the 23rd International Laser Radar Conference, Nara, Japan, 2006*.
- [5] Turner, D.D., B.M. Lesht, S.A. Clough, J.C. Liljegren, H.E. Revercomb, and D.C. Tobin, 2003: Dry bias and variability in Vaisala radiosondes: The ARM experience. *J. Atmos. Oceanic Technol.*, **20**, 117-132.